



ELSEVIER

Contents lists available at SciVerse ScienceDirect

Comptes Rendus Mécanique

www.sciencedirect.com

Wave propagation within some non-homogeneous continua

Exemples de propagation d'onde dans un milieu continu non homogène

Nirmal Antonio Tamarasselvame*, Manuel Buisson, Lalaonirina R. Rakotomanana

Université européenne de Bretagne, IRMAR – université de Rennes 1, campus Beaulieu, 35042 Rennes cedex, France

ARTICLE INFO

Article history:

Received 15 December 2010

Accepted after revision 13 September 2011

Available online 2 October 2011

Keywords:

Waves

Continuum mechanics

Weakly continuous medium

Non-homogeneous continuum

Wave equation

Stop-pass frequency

Confluent hypergeometric function

Mots-clés :

Ondes

Milieux continus

Milieu faiblement continu

Milieu non homogène

Équation des ondes

Fréquence de coupure

Confluent hypergéométrique

ABSTRACT

We investigate the elastic wave propagation within a non-homogeneous continuum according to W. Noll. After some preliminaries in geometry approach suggested by E. Cartan, the linear momentum equation of so-called weakly continuous medium is written. A first example illustrates the modal analysis of an axisymmetric non-homogeneous thick tube. The overall solution is the product of an attenuating exponential response with Kummer's functions. The second example deals with a Timoshenko beam involving transversal displacement and angular rotation of section. We observe the presence of various waves with spatial attenuation, either for the displacement or the section rotation, together with the occurring waves at different scale levels.

© 2011 Académie des sciences. Published by Elsevier Masson SAS. All rights reserved.

R É S U M É

Nous nous intéressons à la propagation d'onde élastique à travers un milieu continu non homogène au sens de W. Noll. Après quelques préliminaires sur l'approche géométrique suggérée par E. Cartan, la loi de la quantité de mouvement pour un milieu dit faiblement continu est écrite. Un premier exemple illustre l'analyse modale d'un cylindre, à paroi épaisse, non homogène et axisymétrique. Les solutions analytiques sont sous la forme d'un produit d'une atténuation exponentielle avec des fonctions de Kummer. Un deuxième exemple étudie une poutre de Timoshenko avec un mouvement transversal et rotatif d'une section. Nous observons la présence d'ondes différentes avec atténuation spatiale, que ce soit pour le déplacement ou la rotation de la section, ainsi que celles se produisant à différents niveaux d'échelle.

© 2011 Académie des sciences. Published by Elsevier Masson SAS. All rights reserved.

1. Introduction

Wave propagation experiments within particular material samples generally emphasize attenuation of the amplitude of the wave: ultrasonic in polycrystalline e.g. [1], micro-porous ceramics e.g. [2], scattering mechanism e.g. [3] and pass band effects in fractured steels plates e.g. [4]. Experimental analysis of wave characteristics within fractured solids, geophysical material, defected material also constitutes an active research field in the domain of non-destructive testing and needs supporting of rigorous underlying concept. Namely the existence of stop-pass band behavior waves which propagate within

* Corresponding author.

E-mail addresses: nirmal.antonio-tamarasselvame@univ-rennes1.fr (N. Antonio Tamarasselvame), manuel.buisson@univ-rennes1.fr (M. Buisson), lalaonirina.rakotomanana-ravelonarivo@univ-rennes1.fr (L.R. Rakotomanana).

such material is an important help in monitoring the in situ degradation of material e.g. [4]. The dispersive character of waves experimentally observed can be analyzed with a higher accuracy but often empirically. Indeed it is usual to a fortiori multiply the wave results of homogeneous medium by an attenuation of the exponential type $\exp(-\alpha x)$ to fit theory with experiments. Additionally, the experimental eigenfrequencies ω_n for some non-homogeneous medium are in general slightly higher than for homogeneous medium e.g. [1]. The classical form of wave propagation equation does not account for the attenuation of the wave, emphasized with the experiments. These materials are named “non-homogeneous”.

Natural definition of “non-homogeneous” means generally that the mass density is variable conversely in homogeneous medium where it may be constant at any point. By this way, for examples, Raj and Sujith [5] reformulated the wave equation for propagation within medium with variable area, Theotokoglou and Stampoulglou [6] considered variable Young’s modulus for investigating on the stress. Such approaches of non-homogeneous medium essentially focus on the distribution of the matter in the medium. In the present study, we focus on the existence of inhomogeneity fields in a material body named “continuum”.

In 1909, Cosserat continuum model was introduced by Cosserat brothers and consists in a continuum model involving independent field of rotation, as primal variable, in addition to the displacement. For many years, Cosserat continuum was used to model non-homogeneous medium e.g. [7]. By using homogenization method and asymptotic analysis, Cosserat continuum models succeed to obtain effective properties of non-homogeneous material. Inspired by this approach, Cartan [8] developed an extended continuum including not only the metric \mathbf{g} for measuring the shape change but also an affine connection ∇ which underlines the gradient operator for tensor field on the continuum; to any affine connection are associated tensors of torsion \mathfrak{N} and curvature \mathfrak{R} which are not necessarily null. In this case, there is a loss of affine equivalence of the material manifold (continuum) with the ambient Euclidean space, corresponding to so-called nonholonomic deformation of the continuum. This provides new motivations for investigating the presence of inhomogeneity field in the continuum from a theoretical point of view e.g. [9–11]. The concept of Cartan circuit was proved by earlier studies of Bilby and Smith [12], Kondo [13], Kröner [14] to bring new insights for modeling continuous distribution of dislocations and disclinations in the continuum. Within the framework of simple material, in [9] Noll gives a new definition of “homogeneous”, and consequently “non-homogeneous”: a material manifold is homogeneous if it exists a configuration (state of deformation of material manifold) in which the mass density, for example, is constant at any point. By this way, an extended class of non-homogeneous continuum called “weakly continuous medium” (WCM) was developed in 1997 by Rakotomanana [15], allowing discontinuities of scalar fields and vectorial fields described by torsion and curvature. The introduction of the torsion as additional kinematical variable can be considered as an extended Cosserat continuum model e.g. [16].

In the present study, we consider then a continuum with inhomogeneity field, in the sense that the distribution of the matter is assumed continuous but that discontinuity of scalar fields (density, temperature, ...) and discontinuity of vectorial fields (velocity, micro-cracks, intergranular decohesion, ...) may appear in the continuum. The “inhomogeneity field” represents both types of discontinuity assumed sufficiently high to accept a continuous volume distribution of inhomogeneity in the continuum. According to the previous definition of Noll, a continuum with inhomogeneity field is named a “non-homogeneous” continuum. We aim to develop an example of WCM for analyzing the wave propagation within a non-homogeneous continuum with only discontinuity of scalar fields. The linear momentum equation was first derived from the equations of Cauchy in a continuum with inhomogeneities e.g. [17], then we analytically solved it for two non-homogeneous samples: a thick-walled cylinder and a Timoshenko beam. The modal analysis aims at describing the presence of a stop-pass frequency and wave attenuation in space, both directly related with the parameter introduced to describe the inhomogeneity field.

2. Preliminary in geometry

A continuum is a set of material points M , modeled by a Riemannian manifold (endowed with a metric \mathbf{g} and an affine connection ∇) which is embedded into Euclidean ambient space E (Cartesian). The transformation of continuum is a map φ from an initial configuration \mathcal{B}_0 , assumed without inhomogeneity field, to its deformed configuration \mathcal{B} : the location of $M \in \mathcal{B}$ is defined by $\mathbf{OM} = \varphi(\mathbf{OM}_0)$ with $M_0 \in \mathcal{B}_0$. The deformation of continuum is then observed with respect to a basis embedded in the continuum. A tangent local base $(\mathbf{f}_{01}, \mathbf{f}_{02}, \mathbf{f}_{03}) \in T_{M_0}\mathcal{B}_0$ is transformed into a deformed base $(\mathbf{f}_1, \mathbf{f}_2, \mathbf{f}_3) \in T_M\mathcal{B}$ according to $\mathbf{f}_a = d\varphi(\mathbf{f}_{0a})$ for $a = 1, 2, 3$, where $d\varphi$ is called the deformation gradient but in general it is not a gradient. Indeed, if the transformation φ is not a diffeomorphism, the notion of gradient is not rigorously defined.

Let $\mathbf{X} \in \mathcal{B}$ a point of the manifold, and let consider a mapping which associates \mathbf{X} to a point of the Euclidean space $\mathbf{x} \in E$. We denote this mapping $\mathbf{x}(\mathbf{X})$ for simplifying. For the sake of the simplicity, we assume that the coordinates $\mathbf{X} = (X^1, \dots, X^n)$ are Cartesian. In the following, we note $(\partial[\dots]/\partial X^k) = [\dots]_{,k}$ and $(\partial[\dots]/\partial X^k \partial X^l) = [\dots]_{,kl}$.

2.1. Holonomic mapping

Let us consider a smooth and single valued mapping: it is a diffeomorphism and we call it holonomic mapping e.g. [17,18]. It is usual to define the deformation gradient also called basis triads (let recall in general case that is not a gradient) in components form, together with its reciprocal basis triads: $F_{\alpha}^i(\mathbf{X}) := x_{,\alpha}^i(\mathbf{X})$ and $F_j^{\beta}(\mathbf{x}) := X_{,j}^{\beta}(\mathbf{x})$. The triads satisfy the orthogonality and the completeness relationships: $F_{\alpha}^i(\mathbf{X})F_i^{\beta}[\mathbf{x}(\mathbf{X})] = \delta_{\alpha}^{\beta}$ and $F_{\alpha}^i(\mathbf{X})F_j^{\alpha}[\mathbf{x}(\mathbf{X})] = \delta_j^i$. We may write the vector

transformation and the components of the metric tensor, where $\hat{\mathbf{e}}_i$ is a vector rigidly attached to the Euclidean space E : $\mathbf{e}_\alpha = F_\alpha^i \hat{\mathbf{e}}_i$ and $\mathbf{g}_{\alpha\beta} = \mathbf{g}(\mathbf{e}_\alpha, \mathbf{e}_\beta)$. On the one hand, since the transformation $\mathbf{x}(\mathbf{X})$ is smooth and single valued, it is integrable, i.e. its derivative commute, by using the classic Schwarz's integrability conditions: $F_{\alpha,\beta}^i - F_{\beta,\alpha}^i = x_{,\beta\alpha}^i - x_{,\alpha\beta}^i = 0$. On the other hand, we can differentiate the vector base:

$$\mathbf{e}_{\alpha,\beta} := \Gamma_{\alpha\beta}^\gamma \mathbf{e}_\gamma = F_{\alpha,\beta}^i \hat{\mathbf{e}}_i = F_{\alpha,\beta}^i F_i^\gamma \mathbf{e}_\gamma \implies \Gamma_{\alpha\beta}^\gamma = F_{\alpha,\beta}^i F_i^\gamma$$

Then it is straightforward to check that the torsion tensor projected in (\mathbf{e}_α) , e.g. [17], is equal to zero during an holonomic transformation: $\aleph_{\alpha\beta}^\gamma := \Gamma_{\alpha\beta}^\gamma - \Gamma_{\beta\alpha}^\gamma = (F_{\alpha,\beta}^i - F_{\beta,\alpha}^i) F_i^\gamma = 0$.

2.2. Nonholonomic mapping and torsion

Now, let consider mapping that are not smooth and/or not single valued. In such a case, the basis triads are not integrable. However, it is possible to map the points surrounding \mathbf{X} defined by the tangent vector $d\mathbf{X}$ to the vector $d\mathbf{x}$ via an infinitesimal transformation defined by the triads: $\mathbf{e}_\alpha = F_\alpha^i \hat{\mathbf{e}}_i$ and $dx^i = F_\alpha^i dX^\alpha$, in which the coefficients functions $F_\alpha^i(\mathbf{X})$ are not integrable in the sense of

$$F_{\alpha,\beta}^i - F_{\beta,\alpha}^i = x_{,\beta\alpha}^i - x_{,\alpha\beta}^i \neq 0$$

In such a case, the mapping is called nonholonomic. It is necessary to modify slightly the previous development to give (the base $\{\hat{\mathbf{e}}_1, \dots, \hat{\mathbf{e}}_n\}$ is assumed rigidly attached to the Euclidean space): $\aleph_{\alpha\beta}^\gamma := \Gamma_{\alpha\beta}^\gamma - \Gamma_{\beta\alpha}^\gamma = (F_{\alpha,\beta}^i - F_{\beta,\alpha}^i) F_i^\gamma \neq 0$, showing that the torsion tensor is not equal to zero for such a nonholonomic mapping. It does not lead to a single valued mapping $\mathbf{x}(\mathbf{X})$. Such a transformation may capture the translational dislocations of Volterra e.g. [11]. This short section permits us to highlight the role of torsion tensor on the classification of continuum transformations. More general proof may be found in a previous work [15], devoted to the class of WCM. More general study on nonholonomic transformation is done in [19], according to [17,18], where notably the role of the curvature tensor \mathfrak{R} is also highlighted. Indeed, torsion tensor is associated to translational dislocations or also to the local discontinuity of any scalar field on the continuum, while curvature tensor is associated to the rotational dislocations or also to the local discontinuity of any vector field on the continuum [15]. In this paper only local discontinuity of scalar field on the continuum will be taken into account.

3. Wave propagation equation

The present section uses the notations introduced in the previous section.

3.1. Kinematics

In continuum mechanics, the Lie–Jacobi bracket $[\mathbf{u}, \mathbf{v}]$ defined for two vector fields, measures the failure of closure of a parallelogram (initially closed). This happens when the continuum deformation includes the nucleation of micro-cracks or the occurrence of dislocations within crystalline solids (see [17] and also [16]). For the Lie–Jacobi bracket no Riemannian metric is required. Let $(\mathbf{f}_{01}, \mathbf{f}_{02}, \mathbf{f}_{03})$ such that $[\mathbf{f}_{0a}, \mathbf{f}_{0b}] = 0$ for $a, b = 1, 2, 3$. If the transformation φ is a C^∞ diffeomorphism then $[\mathbf{f}_a, \mathbf{f}_b] = 0$, e.g. [17]. Otherwise we define the Cartan constants of structure \aleph_{0ab}^c as $[\mathbf{f}_a, \mathbf{f}_b] = \aleph_{0ab}^c \mathbf{f}_c$. The constants of structure \aleph_{0ab}^c characterize the “irreversible” part of the deformation compared to a strongly continuous transformation for which these coefficients remain null if they were initially chosen null. Nevertheless, two bases which can be used for the equation of motion: (a) Coordinate base $(\mathbf{f}_1, \mathbf{f}_2, \mathbf{f}_3)$ which is a local base associated with a curvilinear coordinate system and $\aleph_{0ab}^c = 0$ for $a, b = 1, 2, 3$ (see theorem of Frobenius e.g. [20]); (b) Noncoordinate base $(\mathbf{f}_1, \mathbf{f}_2, \mathbf{f}_3)$ which is not a local base associated with a curvilinear coordinate system and $\aleph_{0ab}^c \neq 0$. The previous subsection on nonholonomic mapping has been presented in noncoordinate base for the sake of simplicity, thus the components of torsion are reduced to the skew-symmetric part of the connection. In general case, the constants of structure are related with the components of the torsion by $\aleph_{ab}^c := \Gamma_{ab}^c - \Gamma_{ba}^c - \aleph_{0ab}^c$, where $\Gamma_{ab}^c := \mathbf{f}^c(\nabla_{\mathbf{f}_a} \mathbf{f}_b)$ represent the coefficients of the (general) affine connection, e.g. [17].

The definition of the deformation faces difficulties in a physically reasonable manner notably when inhomogeneity field grows up within the continuum e.g. [9,10]. For continuum undergoing only holonomic deformation, the deformation of continuum is defined with an Euclidean connection labeled $\bar{\nabla}$ deriving from the Euclidean metric \mathbf{g} and the displacement \mathbf{u} is admitted as primal variable. The metric tensor imposed by the ambient space is $\mathbf{g} = \mathbb{I} + \bar{\nabla} \mathbf{u} + \bar{\nabla}^T \mathbf{u} + \bar{\nabla}^T \mathbf{u} \bar{\nabla} \mathbf{u}$; for small displacement the Cauchy strain $\varepsilon := (1/2)(\bar{\nabla} \mathbf{u} + \bar{\nabla}^T \mathbf{u})$ is related to its linear part, e.g. [21]. In presence of nonholonomic deformation, it is no more possible to describe this deformation by only the metric, the material loosing its affine equivalence with the Cartesian ambient space. Thus, determination of ε faces conceptual problem since the affine connection takes the form of $\nabla = \bar{\nabla} + \nabla^{inh}$ (“inh” for inhomogeneity) where ∇^{inh} is not skew-symmetric with respect to the lower indices e.g. [16,20] (associated torsion is not equal to zero). When undergoing nonholonomic deformation, the kinematics of non-homogeneous continuum includes then the torsion in addition to metric e.g. [19]. Conversely to second grade models e.g. [22], we work here with a tensor metric and separately an affine connection (with torsion) which captures the inhomogeneity field e.g. [9]. In summary, the motion of \mathcal{B} is completely described by the time evolution of the displacement $\mathbf{u}(M, t)$ and the torsion $\aleph(M, t)$. In the following, the connection $\bar{\nabla}$ is employed and consequently we use the Cartan

coefficients of structure: there are 27 non-independent skew-symmetric coefficients $\mathfrak{K}_{0ab}^c = -\mathfrak{K}_{0ba}^c$. Originally proposed by Cartan [8], a 1-form is then defined as $\tilde{\mathfrak{K}}_0 := \mathfrak{K}_{0ab}^a \mathbf{f}^b$ that is a covariant vector which can be considered as a surface-like vector. The non-homogeneous continuum thus consists in a collection of small piece of Euclidean granules, originally called “microcosms” by Gonseth [23]: all of them can deform, translate and rotate with respect to each other (that is the link with the Cosserat model).

3.2. Linear momentum equation

Among the set of equations governing continuum in mechanics, the conservation laws mainly account the conservation of mass, the conservation of linear momentum, the conservation of angular momentum and the conservation of energy. Some authors such as Noll [9] and Kröner [24] have reformulated the classical equilibrium equations of Cauchy for deformed continuum. Conforming to these works, Rakotomanana [17] have attempted to rederive the conservation equations in thermomechanics for non-homogeneous continuum, particularly, the divergence operator must be reshaped accordingly (see [17]). In this paper, we only focus on the linear momentum equation, like conservation law of WCM which is given by e.g. [17,24]:

$$\overline{\text{div}}(\sigma) + \sigma(\tilde{\mathfrak{K}}_0) = \rho \frac{\partial^2 \mathbf{u}}{\partial t^2} \quad (1)$$

The left hand side of (1) includes a classical divergence of the stress $\overline{\text{div}}(\sigma)$ and a contribution of the inhomogeneity field e.g. [17,24] which is source of internal stresses. The theories of elastic or elastic–plastic continuum were developed by accounting for dislocations and disclinations either in the framework of strain gradient e.g. [25–27], or in the context of affinely connected manifold with torsion e.g. [9,10,15,28,29]. The extra term $\sigma(\tilde{\mathfrak{K}}_0)$ captures the stress contribution of inhomogeneity field and attributed to so-called configurational forces e.g. [11,30,31]. This term changes not only quantitatively but also qualitatively the wave propagation e.g. [32]. In the present study, we emphasize the role of the Cartan 1-form $\tilde{\mathfrak{K}}_0$ with the help of simple examples with some reasonable assumptions. For each Euclidean granules (microcosm) constituting the non-homogeneous set, the constitutive law is linear elastic isotropic with a constant mass density $\rho = \rho_0$. And we consider a uniform Cartan 1-form (a vector in an orthonormal base): $\tilde{\mathfrak{K}}_0$ does not depend on the time nor the space. We aim to highlight the effects of simple defects distributed throughout the material on the wave propagation within. A more general form of $\tilde{\mathfrak{K}}_0$ may be considered for further extension of this model. The space gradient of the displacement being $\overline{\nabla} \mathbf{u}$, the Cauchy strain remaining $\varepsilon := (1/2) (\overline{\nabla} \mathbf{u} + \overline{\nabla}^T \mathbf{u})$, we consider the following constitutive law $\sigma = \lambda_0 \text{Tr} \varepsilon \mathbb{I} + 2\mu_0 \varepsilon$, where λ_0 and μ_0 are constants of Lamé. Consequently, from (1) we obtain:

$$(\lambda_0 + \mu_0) \overline{\nabla}(\overline{\text{div}} \mathbf{u}) + \mu_0 \overline{\Delta} \mathbf{u} + \lambda_0 \text{Tr} \varepsilon \tilde{\mathfrak{K}}_0 + 2\mu_0 \varepsilon(\tilde{\mathfrak{K}}_0) = \rho_0 \frac{\partial^2 \mathbf{u}}{\partial t^2} \quad (2)$$

For $\tilde{\mathfrak{K}}_0 = 0$, Eq. (2) reduces to the classical Navier’s equation. The role played by the parameter $\tilde{\mathfrak{K}}_0$ in the resolution of (2) aims to be defined in the next subsection.

For comparison, similar presence of the torsion tensor \mathfrak{K} in the Euler–Lagrange equations is also observed for classical and quantum particle mechanics [18]. Namely the torsion tensor is introduced by means of the space connection whenever nonholonomic path is followed by particles in the space. Also, in a series of papers, Capuani and Willis [33] introduce the wave propagation within discrete models of cracks within otherwise virgin matrix. By considering a random distribution of discrete micro-cracks, and by averaging the crack effects, the equation of wave propagation may be written as follows:

$$(\lambda_0 + \mu_0) \overline{\nabla}(\overline{\text{div}} \mathbf{u}) + \mu_0 \overline{\Delta} \mathbf{u} + \kappa = \rho_0 \frac{\partial^2 \mathbf{u}}{\partial t^2} \quad (3)$$

Where an extra-body force κ in the virgin matrix, due to the presence of micro-cracks distribution appears. Details of the formulation of this extra-body force may be found elsewhere [33].

More generally, constitutive laws of linear elastic solids with distribution of dislocations and disclinations, an example of WCM (see [15]), are obtained by choosing free energy functions depending on higher order of the strain gradients, most of them were derived from original potential proposed by Mindlin e.g. [34]. Such models of first strain gradient, e.g. [22], have been used to describe the inhomogeneity field in continuum and the wave dispersion. Particularly, gradient-enriched elasticity models have been used to investigate the attenuation of high-frequency waves. Such a first strain gradient model does not respect the invariance principle of fields in physics, consequently some forms of potential energy, according to non-Riemannian geometry, are proposed in [19]. But hereafter, we choose an energy without gradient term and we thus note the distinction between the used constitutive law and the conservation law: the constitutive law is linear elastic isotropic homogeneous with constant mass density ρ_0 , while the linear momentum equation is derived from a non-homogeneous continuum, with discontinuity of scalar fields represented by Cartan 1-form $\tilde{\mathfrak{K}}_0$, then considered as a gradient model.

3.3. Stop-pass frequency

Stop-pass frequency originates from 1-D wave propagation through a continuum with micro-fracture distribution, perpendicular to the wave direction, that presents a sound basis for determining the micro-fracture characteristics as geophysics

and mining engineering e.g. [4]. For further simplification, let us consider a fixed-fixed beam of length ℓ for which the kinematics is assumed to be described by a displacement vector $\mathbf{u} := u(x, t) \mathbf{e}_1$ and a uniform Cartan 1-form $\tilde{\mathfrak{N}}_0 := \mathfrak{N}_0 \mathbf{e}_1$ which is similar to the discontinuity of scalar field (inhomogeneity of material) developed in e.g. [17]. The longitudinal velocity is $c_L^2 := (\lambda_0 + 2\mu_0)/\rho_0$, the transversal velocity $c_T^2 := \mu_0/\rho_0$ and the ratio $c^2 := c_T^2/c_L^2 < 1$. Let us introduce the relations $t = T\tilde{t}$, $x = L\tilde{x}$ and $\mathfrak{N}_0 = 2\tilde{\mathfrak{N}}_0 L^{-1}$ where T (time) and L (space) are scales; we choose $T = L/c_L$ and $L = \ell$. For convenience, we will write the non-dimensional variables without over-line. The non-dimensional 1-D wave propagation equation from (2) takes the form of

$$\frac{\partial^2 u}{\partial x^2} + 2\mathfrak{N}_0 \frac{\partial u}{\partial x} - \frac{\partial^2 u}{\partial t^2} = 0 \tag{4}$$

The dynamic equation includes then an additional term $2\mathfrak{N}_0(\partial u/\partial x)$ which represents the influence of inhomogeneity due to the presence of discontinuity of scalar field. This equation looks like a linear damped Klein–Gordon waves equation e.g. [35], dimensionless and with uniform \mathfrak{N}_0 . Eq. (4) can be solved by applying the integral Fourier transform over the dimensionless time t . Assuming $u(x, \cdot) \in H^1(\mathbb{R}) \forall x \in [0, 1]$ and multiplying Eq. (4) by $e^{-i\omega t}$ (ω being an arbitrary parameter, $i^2 = -1$) and integrating it by $\int_{\mathbb{R}} dt$, we obtain a second-order differential equation

$$U''(x) + 2\mathfrak{N}_0 U'(x) + \omega^2 U(x) = 0 \tag{5}$$

where $U(x) := \int_{\mathbb{R}} u(x, t) e^{-i\omega t} dt$ is the Fourier transform of $u(x, \cdot)$. Searching for solutions of the type $U = e^{kx}$, $k \in \mathbb{C}$ (eigenvalues problem), Eq. (5) leads to the dispersion equation $k^2 + 2\mathfrak{N}_0 k + \omega^2 = 0$. Three types of solution k are possible according to the sign of the discriminant $\Delta := \mathfrak{N}_0^2 - \omega^2$. In each case the solution depends on parameters ω and \mathfrak{N}_0 . Given $\omega = \omega_n \in \mathbb{R}_+$, $n = 0, \dots, \infty$ (discrete spectrum), we have a discrete family of solutions k_n . Consequently the solution of (5) takes the form of $U_n(x) = e^{k_n x}$, which finally depends on the parameter \mathfrak{N}_0 . The general solution $u(x, t)$ of wave propagation equation (4) is the decomposition in Fourier series $u(x, t) = \sum_{n \in \mathbb{N}} U_n(x) e^{i\omega_n t}$. We henceforth seek solutions of the type $u(x, t) = U(x) e^{i\omega t}$ in the next examples. We call stop-pass frequency (or cut-off frequency) the frequency ω which is defined by $\Delta = 0$ e.g. [4], $\omega_n \in \mathbb{R}_+$ represents the n th eigenfrequency of the wave, k_n represents the wave number and U_n is the wave function. Let us consider a preliminary example treated in [17] with exactly the same equation as Eq. (4): a fixed-fixed beam of length $l = L$ with discontinuity of scalar field, the boundary conditions are then $U(0) = U(1) = 0$. We should assume $\omega > \mathfrak{N}_0$ since no nontrivial solutions are possible when $\Delta \geq 0$. Indeed when the frequency reaches $\omega \leq \mathfrak{N}_0$, the boundary conditions induce $U_1 = U_2 = 0$, meaning that no waves are allowed to propagate through the non-homogeneous beam. In this paper, the parameter \mathfrak{N}_0 being uniform (no dependence on time nor space), it plays the role of a simple single stop-pass frequency.

4. Applications

4.1. Thick-walled tube

Let us consider a thick-walled tube (cylinder) of infinite length, with inner radius p and outer radius q ($0 < p < q$) in an axisymmetric problem ($\partial_\theta = 0$) with the displacement $\mathbf{u} = u(r, t) \mathbf{e}_r$ and $\tilde{\mathfrak{N}}_0 = \mathfrak{N}_0 \mathbf{e}_r$. For convenience, let us introduce the variables $t = T\tilde{t}$, $r = R\tilde{r}$ and $\mathfrak{N}_0 = 2\tilde{\mathfrak{N}}_0 R^{-1}$, where T and R are scales. Then we chose the following time scale $T = R/c_L$. Again, we will note the non-dimensional variables without over-line. The non-dimensional equation (2) reduces to

$$\frac{\partial^2 u}{\partial r^2} + \left(2\mathfrak{N}_0 + \frac{1}{r}\right) \frac{\partial u}{\partial r} + \left(\frac{2(1 - 2c^2)\mathfrak{N}_0}{r} - \frac{1}{r^2}\right) u = \frac{\partial^2 u}{\partial t^2} \tag{6}$$

Introducing solution type $u(r, t) = U(r) e^{i\omega t}$, $\omega \in \mathbb{R}_+$ for $r \in [p/R; q/R]$ and $t \in [0; +\infty]$, we have

$$U''(r) + \left(A_0 + \frac{B_0}{r}\right) U'(r) + \left(A_1 + \frac{B_1}{r} + \frac{C_1}{r^2}\right) U(r) = 0 \tag{7}$$

where $A_0 = 2\mathfrak{N}_0$, $B_0 = 1$, $A_1 = \omega^2$, $B_1 = 2(1 - 2c^2)\mathfrak{N}_0$, $C_1 = -1$. The general solution of (7) takes then the form of

$$U(r) = r^{-A} e^{-f(r)} [K_1 \mathcal{M}(a, b; h(r)) + K_2 \mathcal{U}(a, b; h(r))] \tag{8}$$

where $\mathcal{M}(\dots; \dots)$ and $\mathcal{U}(\dots; \dots)$ are respectively the Kummer's functions of first and second kind, where $f(r) = a_1 r$ and $h(r) = a_2 r$ and the parameters $A, b, a_1, a_2, a \in \mathbb{C}$ e.g. [36]. Depending of the sign of the discriminant $\Delta := \mathfrak{N}_0^2 - \omega^2$, each set $\{A, b, a_1, a_2, a\}$ corresponds to one base of the solutions of (7). It can be proven that if $\Delta = 0$, the Kummer's functions are defined with help of the Bessel's functions e.g. [37]. If $\Delta < 0$, one of the solutions is

$$A = -1; \quad b = 3; \quad a_1 = \mathfrak{N}_0 + i\sqrt{-\Delta}; \quad a_2 = 2i\sqrt{-\Delta}; \quad a = \frac{-[2(1 - 2c^2)\mathfrak{N}_0 - a_1 - a_2]}{a_2} \tag{9}$$

And if $\Delta > 0$, one of the solutions is

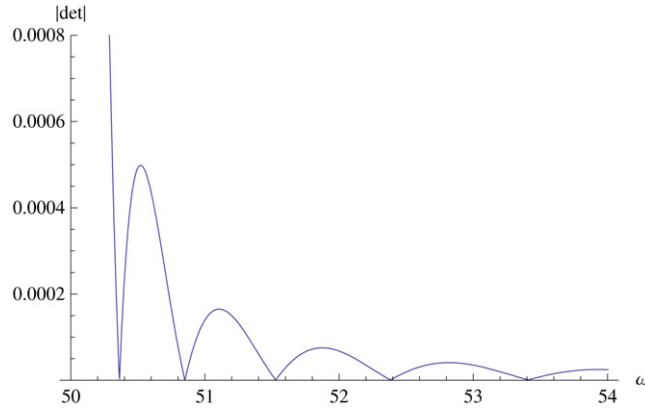


Fig. 1. Norm of the determinant $|\det(\omega, c, r_1)|$ vs. real frequency ω of the non-homogeneous aluminum cylinder.

$$A = -1; \quad b = 3; \quad a_1 = \aleph_0 + \sqrt{\Delta}; \quad a_2 = 2\sqrt{\Delta}; \quad a = \frac{-[2(1 - 2c^2)\aleph_0 - a_1 - a_2]}{a_2} \tag{10}$$

If $\Re(b) > \Re(a) > 0$ then the Kummer’s functions are defined e.g. [37]. We have then chosen parameter $b = 3$. If $\Delta < 0$ we have $\Re(a) = 3/2$ but if $\Delta > 0$, we have $a \in \mathbb{R}$ and the condition $a > 0$ depends on the values of ω , c and \aleph_0 . We cannot correctly define the Kummer’s functions at first sight. Consequently for $\Delta < 0$, the general solution is given with respect to the parameters \aleph_0 , c and ω : $U(r) = r e^{-a_1 r} [K_1 \mathcal{M}(a, 3; a_2 r) + K_2 \mathcal{U}(a, 3; a_2 r)]$. As illustration, let us consider the breathing wave of fixed-fixed cylinder: for an imposed displacement at the two radii $r = p/R$ and $r = q/R$, we have two boundary conditions $U(p/R) = U(q/R) = 0$. We choose $R = p = 50$ [μm] and $q = 100$ [μm], consequently $p/R = 1$, $q/R = 2$. For the convenience of physical interpretation of the inhomogeneity field in the cylinder, we define the characteristic defect length $d_{\aleph} = 2/\aleph_0$ e.g. [17]. The quantity $\aleph_0/2$ (inverse of defect length d_{\aleph}) is the acoustic absorption coefficient e.g. [38]. We choose $d_{\aleph} = 1$ [μm], consequently the dimensional value $\aleph_0 = 2$ [(μm)⁻¹] and the non-dimensional value $\aleph_0 = 50$. For aluminum the velocities $c_L = 3040$ [ms⁻¹] and $c_T = 6420$ [ms⁻¹] e.g. [17]. The boundary conditions hold $U(1) = U(2) = 0$ and then the unknown factors are K_1 and K_2 . Nontrivial solutions exist if and only if the determinant is equal to zero. Since the terms e^{-a_1} and e^{-2a_1} are obviously definite positive, the necessary and sufficient condition reduces to the dispersion equation:

$$\mathcal{M}(a, 3; a_2)\mathcal{U}(a, 3; 2a_2) - \mathcal{M}(a, 3; 2a_2)\mathcal{U}(a, 3; a_2) = 0 \tag{11}$$

which relates the non-dimensional frequency ω , the material properties c , the geometrical shapes (ratio q/R) of the problem and the non-dimensional \aleph_0 . Again, a stop-pass frequency (cut-off frequency) is reached whenever the discriminant $\Delta := \aleph_0^2 - \omega^2$ is equal to zero, i.e. $\omega = 50$. The non-dimensional eigenfrequencies are noted ω_n and represent the values of ω for which both the imaginary and real parts of the determinant (11) are equal to zero. In such a case, the eigenfrequencies ω_n are such that $\omega_n > \aleph_0 = 50$. Fig. 1 permits to capture the eigenfrequencies ($n = 1, \dots, 5$) where the module of the determinant is equal to zero.

We aim to determine a characteristic radius where the wave displacement can be neglected (within non-homogeneous cylinder with $d_{\aleph} = 1$). According to the eigenfrequencies ω_n , $n = 1, \dots, 5$, the wave displacement is $u(r, t) = \sum_{n=1}^5 U_n(r) e^{i\omega_n t}$. Let us consider arbitrary $\epsilon = 10^{-24}$. For $r > 1.1$ we have $|u(r, t)| \leq \sum_{n=1}^5 |U_n(r)| < \epsilon$. Finally the amplitude of the wave is approximately equal to zero within the cylinder for $r > 55$ [μm] (corresponding dimensional radius). This short analysis shows that beyond this radius the wave is strongly attenuated, then the analysis of wave for unbounded continuum is not necessary for such a model.

Now we aim to discuss on the direction of wave. We assume that the displacement \mathbf{u} and the parameter $\tilde{\aleph}_0$ are one-dimensional (with respect to \mathbf{e}_r or \mathbf{e}_θ). We notice the components of the r -depending displacement either $u_r = u(r)$ or $u_\theta = u(r)$. We have investigated the case 1: $\{\mathbf{u} = u(r)\mathbf{e}_r, \tilde{\aleph}_0 = \aleph_0\mathbf{e}_r\}$. Now there are three other following cases: $\{\mathbf{u} = u(r)\mathbf{e}_\theta, \tilde{\aleph}_0 = \aleph_0\mathbf{e}_\theta\}$ (case 2), $\{\mathbf{u} = u(r)\mathbf{e}_r, \tilde{\aleph}_0 = \aleph_0\mathbf{e}_\theta\}$ (case 3) and $\{\mathbf{u} = u(r)\mathbf{e}_\theta, \tilde{\aleph}_0 = \aleph_0\mathbf{e}_r\}$ (case 4). Without accounting for the boundary conditions, Table 1 summarizes the general spatial solution of the wave propagation equation (2), according to the wave \mathbf{u} is parallel (case 1 and case 2) or orthogonal (case 3 and case 4) to inhomogeneity field represented by the scalar $\tilde{\aleph}_0$. All types of the solutions are resumed in Table 1.

4.2. Bending of beam

We investigate a Timoshenko beam, which may be considered as a Cosserat model e.g. [21], with inhomogeneity field. The deformation includes a transversal displacement \mathbf{u} and an angular (vector) rotation θ of a section. Let us introduce the vector \aleph for capturing the inhomogeneity of the material, $\aleph = \aleph_1\mathbf{e}_1 + \aleph_2\mathbf{e}_2$. The kinematics of the beam involves three local fields $(\mathbf{u}, \theta, \aleph)$ at each point \mathbf{x} . We assume rigid transversal section with $\mathbf{u} := -x_2\theta(x_1, t)\mathbf{e}_1 + u_2(x_1, t)\mathbf{e}_2$. From now and

Table 1
Classification of solutions.

$\mathbf{u}/\mathfrak{N}_0$	\mathbf{e}_r	\mathbf{e}_θ
\mathbf{e}_r	Case 1: Confluent hypergeometric functions	Case 3: Bessel first-order + compatibility condition
\mathbf{e}_θ	Case 4: base of solutions: $\{\exp[i(\omega/c)^2 r], \exp[-i(\omega/c)^2 r]\}$	Case 2: Confluent hypergeometric functions

here-after we notice $u_2 := u$ and $x_1 := x$. For convenience, let us introduce the variables $t = T\bar{t}$, $x = L\bar{x}$ and $\mathfrak{N}_1 = 2\bar{\mathfrak{N}}_1 L^{-1}$, where T and L are scales. Then we chose the following time scale $T = L/c_L$. Again, we will note the non-dimensional variables without over-line. Let us note $(\cdot)_{tt} := \partial^2(\cdot)/\partial t^2$, $(\cdot)_x := \partial(\cdot)/\partial x$ and $(\cdot)_{xx} := \partial^2(\cdot)/\partial x^2$. In the following we consider a non-homogeneous beam $\mathfrak{N}_1 \neq 0$ and $\mathfrak{N}_2 = 0$. The system of non-dimensional equations is deduced:

$$\begin{cases} \theta_{xx} + 2\mathfrak{N}_1\theta_x - \theta_{tt} = 0 \\ -(1 - c^2)\theta_x + 2c^2\mathfrak{N}_1(u_x - \theta) + c^2u_{xx} - u_{tt} = 0 \end{cases} \tag{12}$$

in which the first equation is an uncoupled with respect to u . The chosen example is a particular case in which the vector parameter $\mathfrak{N} = \mathfrak{N}_0 \mathbf{e}_1$ [8]. In fact, this is a particular case of Cosserat continuum model, as for micro-polar continuum, rotation θ may occur alone without displacement (as an illustration, a set of aligned domino's falling – with the same motion – on a horizontal table, they relatively slip each other, but the line of mass center remains horizontal) e.g. [34]. In this particular case, the coupling in the first equation disappears. This is not the case when \mathfrak{N} has a component along \mathbf{e}_2 in which coupling terms appear for the two equations constituting the system. It is interesting that this second case, with $\mathfrak{N} = \mathfrak{N}_0 \mathbf{e}_2$, resembles more to the classical Timoshenko beam e.g. [21]. In such a situation, the transverse shear is strongly coupled with the bending as for classical Timoshenko beam. Given $\omega \in \mathbb{R}_+$, searching for solutions of the type $\theta(x, t) = \Theta_0 e^{kx+i\omega t}$ and $u(x, t) = U_0 e^{kx+i\omega t}$, in which $k \in \mathbb{C}$, leads to the system:

$$\begin{cases} k^2\Theta_0 + 2\mathfrak{N}_1k\Theta_0 + \omega^2\Theta_0 = 0 \\ -(1 - c^2)k\Theta_0 + 2c^2\mathfrak{N}_1(kU_0 - \Theta_0) + c^2k^2U_0 + \omega^2U_0 = 0 \end{cases} \tag{13}$$

Nontrivial solutions exist if and only if $(k^2 + 2\mathfrak{N}_1k + \omega^2)(c^2k^2 + 2\mathfrak{N}_1c^2k + \omega^2) = 0$. Two stop-pass frequencies exist for the non-homogeneous bending beam according to the discriminants $\Delta_\theta := \mathfrak{N}_1^2 - \omega^2$ and $\Delta_U := \mathfrak{N}_1^2 - (\omega^2/c^2)$. For each eigenfrequency $\omega_n \in \mathbb{R}_+$, the general form of angular eigenfunctions are easily obtained depending on the value of Δ_θ . Notice that the general solution of (13)₁ is given in respect with the non-dimensional parameter \mathfrak{N}_1 (inhomogeneity of material) and ω (frequency). The second equation gives: $2c^2\mathfrak{N}_1kU + c^2k^2U + \omega^2 U = (1 - c^2)\Theta' + 2c^2\mathfrak{N}_1\Theta$ (with $\Theta = \Theta(x)$ and $U = U(x)$), where the angular eigenfunctions are obtained from (13)₁ and the symbol ' represents the derivative with respect to x . The general transversal solution is the sum of general homogeneous solution and a particular solution: $U(x) = U^{hom}(x) + U^{part}(x)$. For the homogeneous solution we have the three possibilities depending on the value of $\Delta_U := \mathfrak{N}_1^2 - (\omega_n^2/c^2)$. For the particular solution, we have to solve for each $\Theta_n(x)$: $2c^2\mathfrak{N}_1kU + c^2k^2U + \omega^2 U = (1 - c^2)\Theta'_n + 2c^2\mathfrak{N}_1\Theta_n$, in which it is important to consider the previous wave number solution satisfying $k^2 + 2\mathfrak{N}_1k + \omega^2 = 0$. This leads to

$$U_n^{part}(x) = \frac{(1 - c^2)\Theta'_n + 2c^2\mathfrak{N}_1\Theta_n}{-(1 - c^2)\omega_n^2} \tag{14}$$

Let go back to the general case and introduce the both discriminants $\Delta_\theta := \mathfrak{N}_1^2 - \omega^2$ and $\Delta_U := \mathfrak{N}_1^2 - (\omega^2/c^2)$. Since $0 < c^2 < 1$ we have $\Delta_U < \Delta_\theta$. The possible cases are: $\{\Delta_\theta > 0, \Delta_U > 0\}$ and $\{\Delta_\theta > 0, \Delta_U = 0\}$ and $\{\Delta_\theta > 0, \Delta_U < 0\}$ and $\{\Delta_\theta = 0, \Delta_U < 0\}$ and $\{\Delta_\theta < 0, \Delta_U < 0\}$. In the general case, solutions of (13)₂ are determined according to the Δ_U values and the Δ_θ values too. The general solution of (13)₂ is given with respect to the non-dimensional parameters \mathfrak{N}_1 , c and ω . Either for the angle Θ or the displacement U the discriminant cannot be equal to greater or equal to zero since is not compatible with clamped-clamped beam. Indeed, the boundary conditions for a beam of length L ($L = 100$ [μm]) are $\Theta(0) = \Theta(1) = 0$ and $U(0) = U(1) = 0$. They induce $\Theta(x) \equiv 0$ and $U(x) \equiv 0$. This may not be the case for other boundary conditions. For illustration, we consider the bending and transversal wave within a clamped-clamped beam. We thus assume that $\omega > \mathfrak{N}_1$. We have four boundary conditions $\Theta_n(0) = \Theta_n(1) = 0$ and $U_n(0) = U_n(1) = 0$. They lead to the following results represented on Fig. 2 (the material is again aluminum). The wave consists in two distinct contributions: a low frequency wave which supports a higher frequency wave, superimposed on the lower frequency one. For convenience, curves represent only the oscillating aspects of the wave and the attenuation was skipped by dividing the eigenfunctions by $\exp(-\mathfrak{N}_1)$.

We aim to determine a characteristic length where the wave is assumed to be null (within non-homogeneous beam with $d_{\mathfrak{N}} = 1$). According to the eigenfrequencies ω_n , $n = 1, \dots, 5$, the wave angle is $\theta(x, t) = \sum_{n=1}^5 \Theta_n(x)e^{i\omega_n t}$ and the transversal wave is $u(x, t) = \sum_{n=1}^5 U_n(x)e^{i\omega_n t}$. Let us consider arbitrary $\epsilon = 10^{-2}$. For $x > 0.06$ we have $|\theta(x, t)| \leq \sum_{n=1}^5 |\Theta_n(x)| < \epsilon$ and $|u(x, t)| \leq \sum_{n=1}^5 |U_n(x)| < \epsilon$. Finally the amplitude of the total wave (angle and transversal) is approximately equal to zero within the beam for $x > 6$ [μm] (corresponding dimensional length). Here again, we find that it is not necessary to consider unbounded (infinite length) continuum since beyond some characteristic length, the wave is strongly space attenuated.

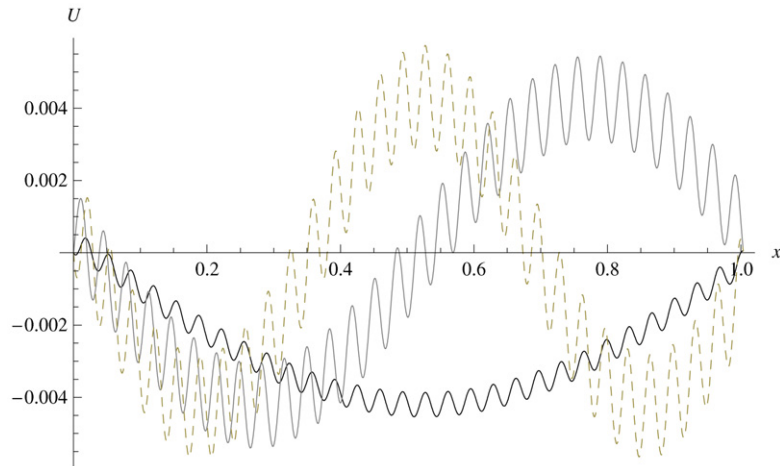


Fig. 2. Three first modal displacement $U_n/\exp(-\aleph_1 x)$ (non-attenuated) for non-homogeneous beam with $d_N = 1$ (plain thick U_1 , plain thin U_2 , dotted U_3).

5. Discussion

The macroscopic wave equation is obtained according to an extended linear momentum equation derived in [15]. The presence of cracks, holes or more generally defects at the mesoscopic level are accounted for by an additional tensorial variable (torsion) to e.g. [9], describing the discontinuity of scalar fields on the continuum due the presence of these defects [17] in classical and quantum physics [18]. The study of wave propagation within non-homogeneous body is conducted in this paper with geometric approach for capturing the inhomogeneities within the material. There are some previous results concerning such a study, that may be compared with this present work. Indeed, for most materials ultrasonic techniques have been developed to characterize the internal degradation by measuring the attenuation of ultrasonic waves. Various theoretical models have been developed for explaining and predicting correlation between attenuation and the presence of micro-cracks e.g. [39]. In the present study, simple micro-cracks are described by a geometric uniform variable \aleph_0 (see [8]).

Basically, attenuation is a collective effect of four contributions e.g. [40]. First, diffraction is a beam spreading that is the dominant source near a crack (wavelength is same order as crack length). Second, far from the crack, absorption (conversion of sound energy to heat) has an exponential relationship of attenuation with distance. It is observed in all case that the wave attenuates exponentially with distance, which typically conforms to the usual absorption contribution e.g. [38,40]. For examples treated in this work, the wave amplitude exponentially decays with respect to the space location beyond small length. These examples were analytically solved, involving confluent hypergeometric functions instead of the classical Bessel's and Hankel's functions (thick-walled tube), and highlighting the occurring of at least two scales for the waves, a higher frequency wave superimposed on a lower frequency wave one (Timoshenko beam). Third, scattering is the dissipation due to geometric dispersion of wave into adjacent media or into non-homogeneity within the material itself. Fourth, velocity dispersion induces a signal loss provoked by the different velocities for different frequencies involved in the wave. Here, the 1-form \aleph_0 field may be considered as variables mimicking small holes deflecting the wave propagation within the sample.

Despite its importance for ultrasonic measurement, most models do not account for attenuation in the initial wave equation. It is often assumed and added ad hoc for fitting with the experimental results e.g. [38,41]. In the present model, the attenuation is accounted for in the initial equation by the extra term $\sigma(\aleph_0)$. For example, experimental analysis of wave propagation in micro-porous ceramics (pores 1 μm) showed strong attenuation and cut-off of frequency e.g. [2]. A sudden decrease in the velocity at high porosity values was shown but could not be explained with macroscopic models of wave propagation. The ability of classical wave propagation to model very micro-porous media was then questioned and the authors assumed that the strong attenuation was due to the wave scattering from the sample geometry disorder than due to the sound adsorption mechanisms in the porous ceramics. Cut-off frequency phenomenon was also observed in macroscopic fractured material, which exhibited distinct frequency bands with energy transmission (pass bands) and with near-zero energy transmission (stop-band with cut-off frequency) e.g. [4]. But here the \aleph_0 being uniform, a single stop-pass frequency is reached for $\|\aleph_0\| = \omega$ and we focused on the eigenfrequencies ω_n . According to [17], when $\|\aleph_0\| \geq \omega$ that corresponds to high density of inhomogeneity, it is equivalent to the situation where the excitation frequency is greater than the defect circular frequency (no wave can propagate). And when $\|\aleph_0\| < \omega$ that corresponds to low density of inhomogeneity and this is the more interesting case. Although experimental measurement techniques are becoming ever more accurate and sophisticated, the list of theoretical models describing micro-cracking detection is still far from complete. Due to the shortness of these micro-cracks characteristic length (1 μm to 10 μm) than the usual wavelength used in ultrasonic techniques, homogeneous linear wave theory has often not sufficiently sensitivity to apprehend material degradation at the mesoscopic level. The present analytic results would serve benchmarks for experimental or numerical simulations.

Furthermore, alternative method for internal variable theory proposes strong discontinuity across the crack lips. Physically, micro-cracks are displacement and/or velocity discontinuities in an otherwise intact material. Indeed, to be close to the physical phenomenon, some micro-mechanics models are based on the physical discontinuity of matter and then assume the description of micro-cracks with contacting lips with dry (or viscous if any) friction at these lips. Each micro-crack is then included into a cell, which is its direct neighborhood and is the smallest unit that allows bulk material properties to be quantified after homogenization. This is the case where the potential energy for each microcosm takes the form of $\mathcal{W}(\varepsilon, \delta_0)$. Similar dependence of the energy on an additional torsion (and also curvature) field is proved in [19] and may give the stress-strain law for non-homogeneous continuum e.g. [21]. The most important properties of the basic cell is the ability to describe the relative translation of contacting lips (cohesion–decohesion) e.g. [42]. The crack opening modes (relative displacements of the crack lips) are the internal variables for these models e.g. [43,44]. Numerous models are based on the discrete distribution of micro-crack within otherwise intact material e.g. [33,43–45].

By this way, the present work is a starting point of new investigations on generalized continuous media.

References

- [1] M. Hirao, H. Ogi, N. Suzuki, T. Ohtani, Ultrasonic attenuation peak during fatigue of polycrystalline copper, *Acta Materialia* 48 (2000) 517–524.
- [2] F. Craciun, G. Guidarelli, C. Galassi, E. Roncari, Elastic wave propagation in porous piezoelectric ceramics, *Ultrasonics* 36 (1998) 427–430.
- [3] D. Grady, Scattering as mechanism for structured shock waves in metals, *J. Mech. Phys. Solids* 46 (10) (1998) 2017–2032.
- [4] S. Nakagawa, K.T. Nihei, L.R. Myer, Stop-pass behavior of acoustic waves in a 1D fractured system, *J. Acoust. Soc. Am.* 107 (1) (2000) 40–50.
- [5] A. Raj, R.I. Sujith, Closed-form solutions for the free longitudinal vibration of inhomogeneous rods, *J. of Sound and Vibration* 283 (2005) 1015–1030.
- [6] E.E. Theotokoglou, I.H. Stampoulouglou, The radially nonhomogeneous elastic axisymmetric problem, *Int. J. of Solids and Struct.* 45 (2008) 6535–6552.
- [7] S. Forest, K. Sab, Cosserat overall modelling of heterogenous materials, *Mechanics Research Communications* 25 (4) (1998) 449–454.
- [8] E. Cartan, *On Manifolds with an Affine Connection and the Theory of General Relativity*, Bibliopolis, Napoli, 1986 (English translation of the French original by A. Magnon and A. Ashtekar).
- [9] W. Noll, Materially uniform simple bodies with inhomogeneities, *Arch. Rat. Mech. Anal.* 27 (1967) 1–32.
- [10] C.C. Wang, On the geometric structure of simple bodies, or mathematical foundation for the theory of continuous distributions of dislocations, *Arch. Rat. Mech. Anal.* 27 (1967) 33–94.
- [11] G.A. Maugin, *Material Inhomogeneities in Elasticity*, Chapman & Hall, 1993.
- [12] B.A. Bilby, E. Smith, Continuous distributions of dislocations: a new application of the method of non-Riemannian geometry, *Proc. Roy. Soc. London A* 231 (1955) 263–273.
- [13] K. Kondo, Non-Riemannian geometry of imperfect crystals from macroscopic view-point, in: *Memoirs of the Unifying Study of Basic Problems in Engineering Sciences by Means of Geometry*, vol. I, Gakujutsu Benken Fukyu-Kai, Division D, Tokyo, 1955.
- [14] E. Kröner, Dislocation: a new concept in the continuum theory of plasticity, *J. Math. Phys.* 42 (1963) 27–37.
- [15] L.R. Rakotomanana, Contribution à la modélisation géométrique et thermodynamique d'une classe de milieux faiblement continus, *Arch. Rat. Mech. Anal.* 141 (1997) 199–236.
- [16] F.W. Hehl, T.N. Obukhov, Elie Cartan's torsion geometry and in field theory, an essay, *Annales de la Fondation Louis de Broglie* 32 (2–3) (2007) 157–194.
- [17] L.R. Rakotomanana, *A Geometric Approach to Thermomechanics of Dissipating Continua*, Birkhäuser, Boston, 2003.
- [18] H. Kleinert, Nonholonomic mapping principle for classical and quantum mechanics in spaces with curvature and torsion, *General Relativity and Gravitation* 32 (5) (2000) 769–839.
- [19] N. Antonio Tamarasselvame, L.R. Rakotomanana, On the form-invariance of Lagrangian function of higher gradient continuum, in: H. Altenbach, G.A. Maugin, V.I. Erofeev (Eds.), *Mechanics of Generalized Continua*, *Adv. Struct. Mater.* 7 (2011) 291–322.
- [20] M. Nakahara, *Geometry, Topology and Physics*, Graduate Student Series Physics, IOP Publishing, 1996.
- [21] L.R. Rakotomanana, *Éléments de dynamique des structures et solides déformables*, Collection Mécanique, Presses Polytechniques et Universitaires Romandes, Lausanne, 2009.
- [22] N.A. Fleck, J.W. Hutchinson, Strain gradient plasticity, in: J.W. Hutchinson, T.Y. Wu (Eds.), *Adv. in Appl. Mech.*, vol. 33, Academic Press, 1997, pp. 295–361.
- [23] F. Gonthier, *Les fondements des mathématiques: De la géométrie d'Euclide à la relativité générale et à l'intuitionisme*, Librairie scientifique et technique Albert Blanchard, Paris, 1926.
- [24] E. Kröner, Continuum theory of defects, in: Balian, et al. (Eds.), *Physique des défauts les Houches*, July 28–August 29, North-Holland Publishing, 1981, pp. 219–315, 27–37.
- [25] K.C. Le, H. Stumpf, On the determination of the crystal reference in nonlinear continuum theory of dislocations, *Proc. R. Soc. London A* 452 (1996) 359–371.
- [26] M.Y. Gutkin, E.C. Aifantis, Dislocations and disclinations in gradient elasticity, *Phys. Stat. Sol. B* 214 (1999) 245–284.
- [27] A. Menzel, P. Stemann, On the continuum formulation of higher gradient plasticity for single and polycrystals, *J. Mech. Phys. Solids* 48 (2000) 1777–1796.
- [28] M. Lazar, An elastoplastic theory of dislocations as a physical field with torsion, *J. Phys. A: Math. Gen.* 35 (2002) 1983–2004.
- [29] S. Deng, J. Liu, N. Liang, Wedge and twist disclinations in second strain gradient elasticity, *Int. J. Solids Struct.* 44 (2007) 3646–3665.
- [30] V. Popov, E. Kröner, On the dynamic theory of elastoplastic medium with microstructure, *Computational Material Sciences* 16 (1999) 218–236.
- [31] M.E. Gurtin, *Configurational Forces as Basis Concepts of Continuum Physics*, Springer, New York, 2000.
- [32] M. Ostoja-Starzewski, A. Woods, Spectral finite elements for vibrating rods and beams with random field properties, *J. of Sound and Vibration* 268 (2003) 779–797.
- [33] D. Capuani, J.R. Willis, Wave propagation in elastic media with cracks. Part II: Transient nonlinear response of a cracked matrix, *Eur. J. Mech. A/Solids* 18 (1999) 159–175.
- [34] R.D. Mindlin, H.F. Tiersten, Effects of couple-stresses in linear elasticity, *Arch. Rat. Mech. Anal.* 11 (1962) 415–448.
- [35] F.K. Kneubühl, *Oscillations and Waves*, Springer Verlag, Heidelberg, 1997.
- [36] N. Challamel, A. Andrade, D. Camotim, An analytical study on the lateral-torsional buckling, *Int. J. Struct. Stabil. Dynam.* 7 (3) (2007) 445–447.
- [37] M. Abramowitz, I.A. Stegun, *Handbook of Mathematical Functions*, Applied Mathematics Series, vol. 55, National Bureau of Standards, 1964, pp. 358, 555.
- [38] M.A. Breazeale, J.H. Cantrell Jr., J.S. Heyman, Ultrasonic wave velocity and attenuation measurements, in: P.D. Edmonds (Ed.), *Methods of Experimental Physics* 19: *Ultrasonics*, Academic Press, Orlando, 1981, pp. 67–135.
- [39] A. Vary, Concepts for interrelating ultrasonic attenuation, microstructure, and fracture toughness in polycrystalline solids, *Materials Evaluation* 46 (5) (1988) 642–649.

- [40] W.H. Prosser, Advanced AE techniques in composite materials research, *J. of Acoustic Emission* 14 (3–4) (1996) S1–S11.
- [41] B. Vandenbossche, R.D. Kriz, T. Oshima, Stress-wave displacement polarizations and attenuation in unidirectional composites: Theory and experiment, *Res. Nondestr. Eval.* 8 (1996) 101–123.
- [42] K.B. Broberg, The cell model of materials, *Computational Mechanics* 19 (1997) 447–452.
- [43] G.A. Maugin, *The Thermomechanics of Plasticity and Fracture*, Cambridge University Press, Cambridge, 1992.
- [44] J. Oliver, M. Cervera, O. Manzoli, Strong discontinuities and continuum plasticity models: The strong discontinuity approach, *Int. J. Plasticity* 15 (1999) 319–351.
- [45] N. Ramaniraka, L.R. Rakotomanana, Models of continuum with micro-crack distribution, *Math. Mech. Solids* 5 (2000) 301–336.